Journal of Statistical Physics, Vol. 54, Nos. 5/6, 1989

Power Spectra and Spatial Pattern Dynamics of a Ring Laser

Anthony W. Yu,[1] Govind P. Agrawal,[2] and Rajarshi Roy[3]

Received March 30, 1988

Experimental measurements of power spectra of a single longitudinal and transverse mode ring dye laser are presented that reveal the critical slowing down of the laser near threshold. External pump noise serves as a probe of the frequency response of the dye laser. Detailed comparisons of the spectral characteristics with computer simulations and an approximate analytic theory are given. The dynamics of spatial pattern formation in a multimode dye laser is examined through measurements of first-passage-time distributions. A comparison of the experiments with computer simulations based on a simple theoretical model of the two-mode laser shows qualitative agreement. These measurements indicate that there are a variety of complex phenomena associated with the transverse mode pattern formation dynamics that need to be addressed theoretically and studied further experimentally.

KEY WORDS: Power spectra; noise; transverse modes; laser dynamics.

1. INTRODUCTION

The problem of random flights and the phenomenon of Brownian motion provided some of the earliest examples for the study of stochastic processes.[1] Lord Rayleigh realized that these questions were formally identical to "that of the composition of n isoperiodic vibrations of unit amplitude and of phases distributed at random."[2] These initial investigations led the way for the development of the theory of stochastic processes and its application to diverse physical and chemical phenomena.[3]

The statistical nature of the electromagnetic fields emitted by light sources, particularly those in the visible, was recognized in numerous

[1] School of Physics, Georgia Institute of Technology, Atlanta Georgia 30332.
[2] AT & T Bell Laboratories, Murray Hill, New Jersey 07974.

0022-4715/89/0300-1223$06.00/0

efforts to quantify notions of the coherence of light.[4] The invention of the laser brought renewed activity to this area, and focused on the necessity to clearly define coherence and differentiate between the light emitted by laser and thermal sources. The early research on the coherence properties of optical fields was reviewed in the classic paper of Mandel and Wolf.[5] The classical and quantum definitions of coherence[6–8] were reconciled in the optical equivalence theorem.[9,10]

The study of the coherence properties of laser light rapidly proved to be an important testing ground for the theory of stochastic processes.[11] In recent years, the study of random phenomena in lasers has revealed the importance of non-Markovian noise sources in the determination of the coherence properties of lasers.[12] The nonlinear character of lasers has also become widely recognized through the discovery and interpretation of a wide variety of chaotic phenomena, many of which had been dismissed earlier as "noise effects" of mysterious origin.[13]

In this paper, we concentrate on random phenomena in lasers that are caused by noise sources; the influence of spontaneous emission and external pump noise will be considered. Though lasers operate primarily through stimulated emission, spontaneous emission from the inverted atoms or molecules is always present, and constitutes an inevitable source of noise. External pump noise is present in secondary lasers that are pumped by other (primary) lasers. The pump noise often has a time scale of fluctuations that is comparable to the times for decay or growth of the secondary laser field, and must then be treated as a non-Markovian noise source. The noise in the primary pump laser intensity affects the population inversion in the secondary laser medium. Such noise is also present when the mechanism for creation of the inversion contains fluctuations, e.g., the injection current fluctuations in semiconductor lasers.[14] Though pump noise can in principle be reduced, there are also fundamental limits to this reduction. Johnson noise provides such a limit in semiconductor lasers. The reduction of pump noise in semiconductor lasers is of considerable importance for the production of squeezed states.[15]

The experimental studies reported here were performed on a ring dye laser (an important example of secondary lasers) pumped by an argon ion laser. The dye laser may be operated in a single longitudinal and transverse mode. It may also be operated such that several longitudinal and transverse modes coexist simultaneously. The laser system is described in Section 2. In Section 3 we will examine power spectral measurements for a single-mode dye laser for a wide range of operating power levels. An approximate analytic solution to the stochastic equations for the laser with additive (spontaneous emission) and multiplicative (external pump) noise sources will be compared with the experimental results. Computer

simulations of the stochastic differential equations verify the accuracy of the analytic results for operation of the laser above threshold, and reveal inadequacies of the approximation near threshold. The power spectra of the dye laser may be represented as a product of two Lorentzians, a form discussed by Sigeti and Horsthemke in a recent paper.[16] These measurements show that the response of the secondary laser to the fluctuations of the primary laser intensity is very sluggish near threshold. Far above threshold, the secondary laser reproduces the pump noise quite faithfully. An interpretation of these observations in terms of the critical slowing down of the dye laser near threshold is given.

Section 4 provides a brief review of the first-passage-time (FPT) concept and its use in the study of noise phenomena in lasers. The application of passage time measurements to multimode lasers is then described. In contrast to the FPT distributions for single-mode lasers, it is found that multimode lasers may display distributions with multiple peaks. In a ring dye laser, these multiple peaks are observed when the laser operates in two or more transverse modes simultaneously. Photographs of steady-state transverse mode profiles are presented, and then the dynamics of the formation of these beautiful spatial patterns are examined through passage time distributions. A qualitative comparison of these distributions with a theoretical model is presented. A discussion and summary of the results is presented in Section 5.

2. EXPERIMENTAL APPARATUS

The experimental apparatus used for the experiments is shown in Fig. 1. A ring dye laser is pumped by an argon ion laser (514.5 nm) that is intensity stabilized with an electro-optic modulator. The electro-optic stabilizer allows us to operate the dye laser near threshold for long periods of time without appreciable drift of the operating point, since the average pump power is maintained constant to within a fraction of a percent. The pump laser fluctuations are reduced, but not eliminated, by the stabilizer. The dye laser is enclosed in a box to minimize air currents and dust. The entire apparatus rests on a vibration-isolated table, and its mode structure is monitored with a confocal Fabry–Perot interferometer to ensure that it is operating in a single mode. A Faraday rotator and compensator are used to obtain unidirectional operation, and intracavity etalons are used to select a single longitudinal mode. For the first-passage-time measurements to be described in Section 4, an acousto-optic modulator (AOM) is introduced into the cavity. To produce one or more higher order modes, the pump mirror was tilted slightly to cause a mismatch between the pump and dye beams within the active medium. The nature of the fluid flow in

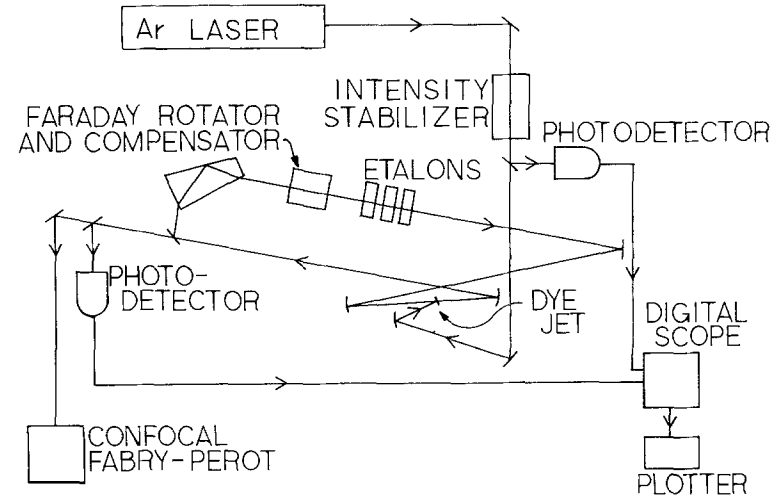

(a)

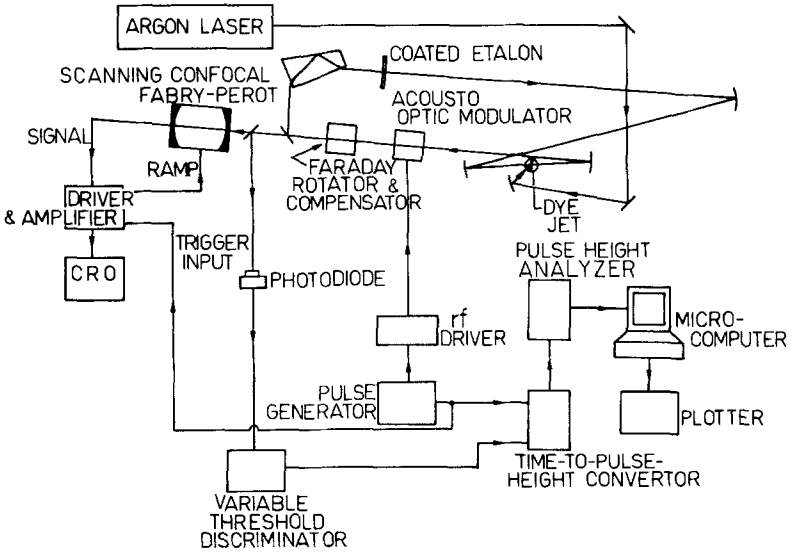

(b)

Fig. 1. (a) Experimental setup for the measurement of power spectra for a single-mode unidirectional ring dye laser. (b) Experimental apparatus for the measurement of first-passage-time distributions for the ring laser. A large-surface-area photodiode ensures that the entire spatial mode is incident on the photosensitive surface.

the dye jet at the spot where it was pumped by the argon laser also affected the spatial mode structures. The transverse mode structure of the laser is monitored by enlarging the beam with a lens and projecting it onto a screen. For the power spectral measurements, two fast photodiodes with <1 nsec risetime were employed. A large-area (EG & G SGD 160) photodiode with a risetime of <7 nsec was used for the passage time measurements on the transverse modes. This is still fast enough for the measurements, and the surface area is large enough to capture the entire beam. The argon laser was used without the intensity stabilizer and with an all-lines mirror for the transverse mode measurements, since a higher pump power is necessary to achieve lasing in one or more higher order transverse modes simultaneously.

In the case of the power spectral measurements, the pump and dye laser outputs were detected and stored in a digital oscilloscope, and fast Fourier transforms (FFT) were performed on the data to yield the power spectra. The power spectrum was averaged several times, and the resulting spectrum displayed. The width of the spectrum can be read off in a prescribed manner and plotted for different points of operation of the laser.

For the passage time measurements, the laser is Q-switched with the AOM and a start pulse input to a time to pulse height analyzer. When the laser output intensity crosses a certain threshold as determined by a discriminator, a stop pulse is input to the analyzer. The output pulse of the analyzer is proportional in height to the time interval between the start and stop pulses, thus giving the first passage time distribution for the laser intensity to reach a desired level. The discriminator threshold can then be set to a different voltage and the entire procedure repeated to obtain the corresponding passage time distribution. The pulse height analyzer output is stored in a microcomputer for later analysis.

3. POWER SPECTRA FOR THE SINGLE-MODE LASER

Initial measurements of power spectra of a single-mode dye ring laser were recently reported by us[17] to describe pump noise propagation from pump to secondary lasers. The dye laser was shown to behave like a low-pass filter near threshold, while above threshold the pump laser fluctuations were reproduced with greater accuracy. Here we report new measurements of power spectra for steady-state operation of the dye laser taken over a wide range of operating points from very near threshold to far above threshold. We compare the widths of these power spectra to those obtained theoretically from an analytic approximation and also from computer simulation of the nonlinear stochastic equations of motion.

The power spectrum of the argon laser was measured, and the full width at half maximum of a Lorentzian fit to the low-frequency portion of the spectrum was determined to be 5×10^4 Hz. This value was used for all the calculations. It should be noted that the argon laser power spectrum is not exactly Lorentzian in shape. Only the low-frequency portion of the spectrum is fitted with the Lorentzian; at higher frequencies there exist peaks in the spectrum which are not taken into account here. However, these peaks are several tens of dB below the zero-frequency value and occur at frequencies well beyond those that determine the low-frequency response of the dye laser to pump fluctuations, and may be assumed negligible for our purpose. The individual power spectra for the dye laser at different operating points are very similar to those shown in ref. 17 and will not be reproduced here. To estimate the width of these power spectra, which decay much faster than a Lorentzian, we chose the value at 30 dB below the zero-frequency value. This is a somewhat arbitrary choice, but is dictated by the fact that the power spectra are almost indistinguishable from each other if the full width at half maximum is taken. This becomes clear also when we examine the spectra from the analytic calculations and simulations.

The equation of the electric field for the dye laser is given by

$$\dot{E} = a_0 E - A\,|E|^2\,E + p(t)\,E + q(t) \tag{1}$$

where $p(t)$ is a colored pump noise term and $q(t)$ is a delta-correlated spontaneous emission noise term. The parameter a_0 is the average net gain of the laser, while A is the saturation coefficient. The statistical properties of the two noise terms are given by

$$\langle q(t)\,q^*(t')\rangle = 2R\delta(t-t') \tag{2}$$

$$\langle p(t)\,p^*(t')\rangle = D\Gamma_p \exp(-|t-t'|\,\Gamma_p) \tag{3}$$

where R and D are the noise strengths of the spontaneous emission and pump fluctuations and $1/\Gamma_p$ is the time scale of the pump noise. To solve this equation numerically, we need a further equation to generate the colored pump noise. The method introduced by Sancho *et al.*[14] was used, and the auxiliary equation

$$\dot{p}(t) = -\Gamma_p p(t) + \Gamma_p q'(t) \tag{4a}$$

$$\langle q'(t)\,q'^*(t')\rangle = 2D\delta(t-t') \tag{4b}$$

was iterated simultaneously with Eq. (1). Since the field and the noise terms are actually complex, we numerically solve the four equations for the real and imaginary components. Since only fluctuations about the steady state are being measured, we allowed the laser intensity to approach steady state

before storing the intensity values on which the FFT was performed to generate the power spectra. The number of steps used was 16,384, and a total of 50 trajectories were averaged over to produce the spectra shown in Fig. 2. The strengths of the noise terms used here are $R = 0.004\ \text{sec}^{-1}$ and $D = 1 \times 10^4\ \text{sec}^{-1}$; these were obtained from FPT measurements on the dye laser,[19] as was the value of $A = 1 \times 10^5\ \text{sec}^{-1}$. The low-pass filter action of the dye laser is clear from Fig. 2, where the power spectra normalized to the value at zero frequency are plotted for several different values of a_0. The parameter a_0 is equal to $G - \kappa$, where G is the gain and κ is the cavity decay rate. For the dye laser used in this experiment, $\kappa = 1 \times 10^7\ \text{sec}^{-1}$. Threshold is defined by the condition $G = \kappa$, and hence $a_0 = 0$. Above threshold, $a_0 = \kappa\eta$, where the relative excitation above threshold is defined as $\eta = G/\kappa - 1$. Thus, $a_0 = 1 \times 10^6\ \text{sec}^{-1}$ corresponds to $\eta = 0.1$, i.e., operation 10% above threshold.

A comparison of theory and experiment is provided in Fig. 3, where we have plotted the widths of the simulated power spectra at the point 30 dB below the zero-frequency value for different values of a_0 as well as those obtained from the experimental measurements. The agreement between the experiment and Monte Carlo calculations (triangles) is quite good, over the entire range of output power from 0.1 to 25 mW. It is seen that the widths of the power spectra saturate at a few mW. The power at

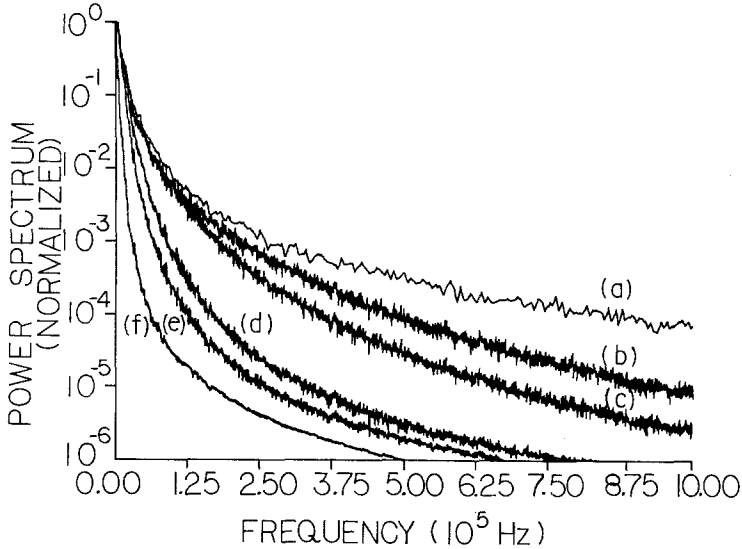

Fig. 2. Power spectra obtained from Monte Carlo simulation of Eqs. (1)–(4). The net gain coefficient a_0 is (a) 1×10^7, (b) 1×10^6, (c) 5×10^5, (d) 1×10^5, (e) 5×10^4, and (f) $5 \times 10^3\ \text{sec}^{-1}$, respectively. The other parameters are $R = 0.004\ \text{sec}^{-1}$, $D = 5 \times 10^3\ \text{sec}^{-1}$, $\Gamma_p = 5 \times 10^4\ \text{sec}^{-1}$, and $A = 1 \times 10^5\ \text{sec}^{-1}$.

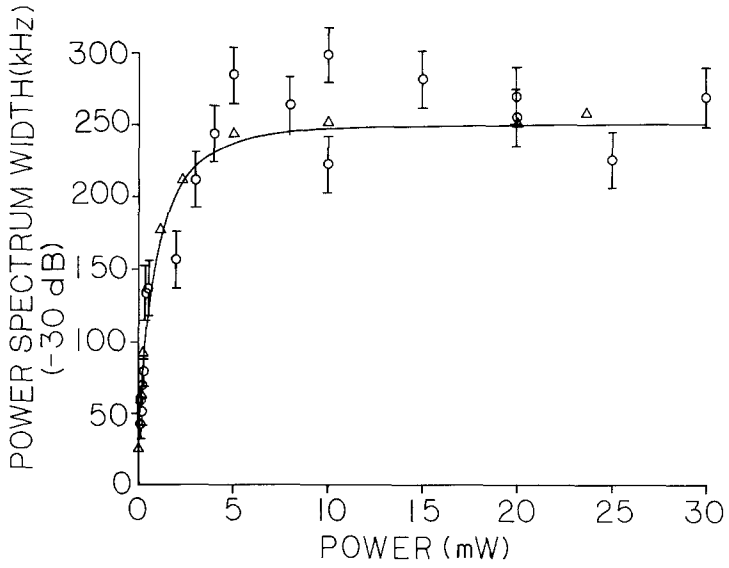

Fig. 3. Comparison of the widths (at -30 dB) of experimentally measured power spectra ($\bigcirc$) and those obtained from the simulations (Δ) and analytic approximation (solid line) of Eq. (9).

which saturation occurs is dependent on the definition of the width of the power spectrum. The solid line shown in the figure is obtained by noting the width of the spectrum (at the -30 dB point) calculated from the analytic approximation described below.

Though analytic solutions for the nonlinear differential equation (1) with colored noise are not available, it is possible to obtain a good analytic approximation to the behavior of the power spectra above threshold if a linearized analysis is performed. Equation (1) can be transformed into one for the laser intensity $I=|E|^2$,

$$\dot{I}=2a_0 I-2AI^2+R+2p_r(t)\,I+2q_r(t)\,I^{1/2} \tag{5}$$

where the subscript r denotes the real part of the complex noise terms. Fluctuations of the intensity about the steady-state average value $\bar{I}(t)$ are denoted by $\delta(t)$, defined through the equation

$$I(t)=\bar{I}(t)+\delta(t) \tag{6}$$

The steady-state average intensity above threshold is given by $\bar{I}=a_0/A$. The differential equation for $\delta(t)$ becomes, upon linearization,

$$\dot{\delta}(t)=\left[2a_0-4A\bar{I}+2p_r(t)+\frac{q_r(t)}{\bar{I}^{1/2}}\,\delta(t)+2q_r(t)\,\bar{I}^{1/2}+2p_r(t)\,\bar{I}\right] \tag{7}$$

If the noise terms in the square bracket are neglected in comparison with $2a_0 - 4A\bar{I}$, the equation may be Fourier transformed and solved for $\tilde{\delta}(\omega)$,

$$\tilde{\delta}(\omega) = \frac{2\bar{I}\tilde{p}_r(\omega) + 2\tilde{q}_r(\omega)\,\bar{I}^{1/2}}{2a_0 + i\omega} \tag{8}$$

where the quantities with tilde are Fourier transforms. The power spectrum of the laser intensity fluctuations is now obtained from Eqs. (2), (3), and (8):

$$S(\omega) = \langle |\tilde{\delta}(\omega)|^2 \rangle = \frac{4\bar{I}R}{\omega^2 + \Gamma_L^2} + \frac{(D/A^2)\,\Gamma_L^2\Gamma_p^2}{(\omega^2 + \Gamma_L^2)(\omega^2 + \Gamma_p^2)} \tag{9}$$

where $\Gamma_L = 2a_0$. The first term is dependent only on the spontaneous emission, and will be negligible above threshold. The second term is the product of two Lorentzians, and demonstrates exactly the same behavior as seen from the direct simulation of the equation for the electric field. Far above threshold, the power spectrum approaches that of the pump laser noise. The Lorentzian of width Γ_L is now much broader than the one with width Γ_p, and it is the latter that determines the shape of the overall spectrum. For operation near threshold, the value of Γ_L approaches Γ_p, and the width of the spectrum becomes much narrower than that of the single Lorentzian for the pump noise.

Several power spectra obtained from Eq. (9) are shown in Fig. 4.

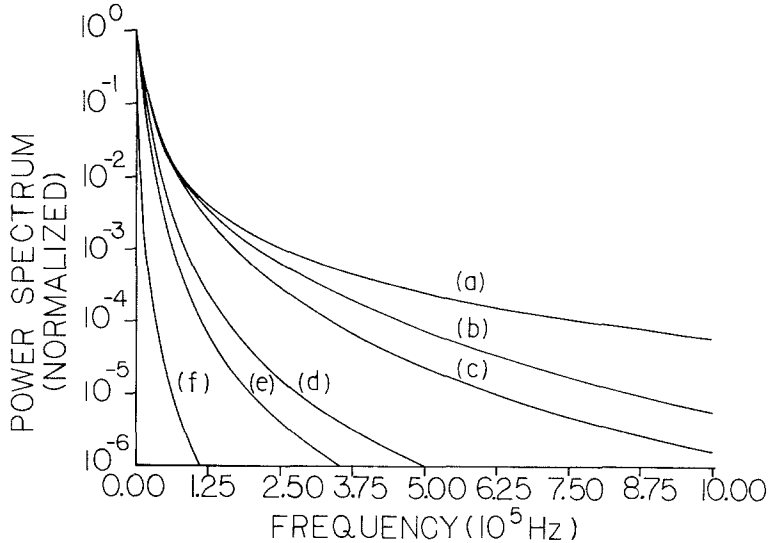

Fig. 4. Power spectra from the analytic approximation in Eq. (9). The values of the net gain coefficient are varied as in Fig. 2 and $\Gamma_p = 5 \times 10^4\ \text{sec}^{-1}$.

A comparison of the curves in Fig. 4 with those of Fig. 2 reveals that there is excellent agreement between the simulations and the analytic approximation for high values of a_0. As a_0 decreases, and the laser is operated closer to threshold, the difference between the solution of the nonlinear equations and the linearized approximation becomes clear. However, even for operation at 0.1% above threshold, the linearized solution reproduces the numerical results quite well, particularly if the widths of the spectra are compared at the -30 dB point. This is obvious from an examination of Fig. 3, where the widths obtained from experiment, simulations, and analytic calculations are all seen to be in good agreement.

The form of the power spectrum in Eq. (9) is identical to one contained in the recent paper by Sigeti and Horsthemke.[15] They derive this form of the power spectrum in a discussion of the differences in power spectra for systems that are chaotic and those that are driven by noise. Our measurements are an example of the latter, and demonstrate exactly the behavior expected for systems driven by colored noise.

The behavior of the dye laser near threshold as a low-pass filter for the fluctuations of the pump laser illustrates the critical slowing down that occurs in the laser. The analogy of the overdamped motion of a particle in a potential well to the laser is well known. The equation for the potential obtained from the equation for $\dot{I}$ [Eq. (5)] is

$$V(I) = -a_0 I^2 + \tfrac{2}{3} A I^3 \tag{10}$$

Near threshold, a_0 is small, and the potential is flat near the origin. The motion of the particle is very slow, and it does not respond to fast fluctuations. This is the phenomenon of critical slowing down. For operation far above threshold, the well of the potential becomes sharp, and the relaxation time for the particle motion becomes much shorter. The particle responds to external fluctuations on a much shorter time scale. In the case of the laser, the response of the secondary laser to fluctuations of the pump laser is slow near threshold and faster above threshold. The external noise functions as a probe of the critical slowing down of the laser near threshold.

In this section we have examined the effect of external noise on the low-frequency fluctuations of the intensity of a single longitudinal and transverse mode ring laser operated in the steady state. We will now proceed to describe our studies of the dynamics of spatial patterns in a multimode laser. The effect of external noise on the time evolution of these patterns is investigated by measurements of the first-passage-time distributions of the laser intensity.

4. SPATIAL PATTERN DYNAMICS IN A MULTIMODE LASER

Spatial patterns in the light emitted by lasers are determined by the resonator or optical cavity that confines the light. Solutions of the wave equation for the resonator under the paraxial approximation are well known and several studies have recorded the spatial patterns corresponding to different transverse modes of the resonator.[20] Numerical techniques for the analysis of resonators consist of propagation of a wavefront through the cavity, subject to the correct boundary conditions until it settles down, and a wavefront that repeats on every round trip in both phase and amplitude is obtained.

The most basic spatial pattern of the radiation from a stable resonator is a two-dimensional Gaussian mode, and the higher order modes are products of Hermite functions in x and y (for a rectangular geometry), the two transverse dimensions, assuming that the z axis is coincident with the beam propagation direction in the cavity.[21] Figure 5 shows several of the higher order spatial modes generated in a dye laser with mirrors of large enough diameter that their cylindrical geometry is ineffective in deter-

(a)

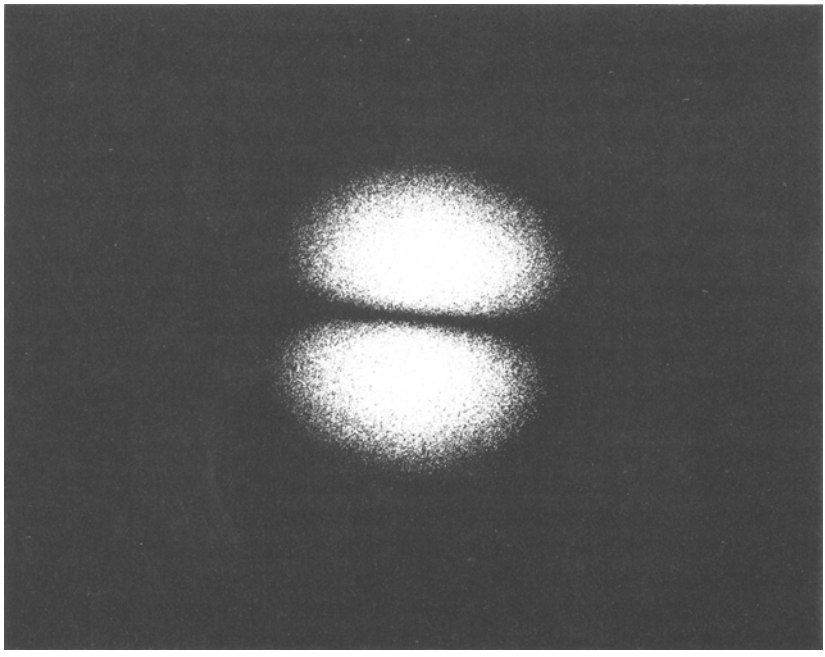

Fig. 5. Higher order spatial modes generated in a dye laser. These modes are respectively (a) $TEM_{1,0}$, (b) $TEM_{2,0}$, (c) $TEM_{3,1}$, (d) $TEM_{3,2}$, and (e) $TEM_{20,0}$.

(b)

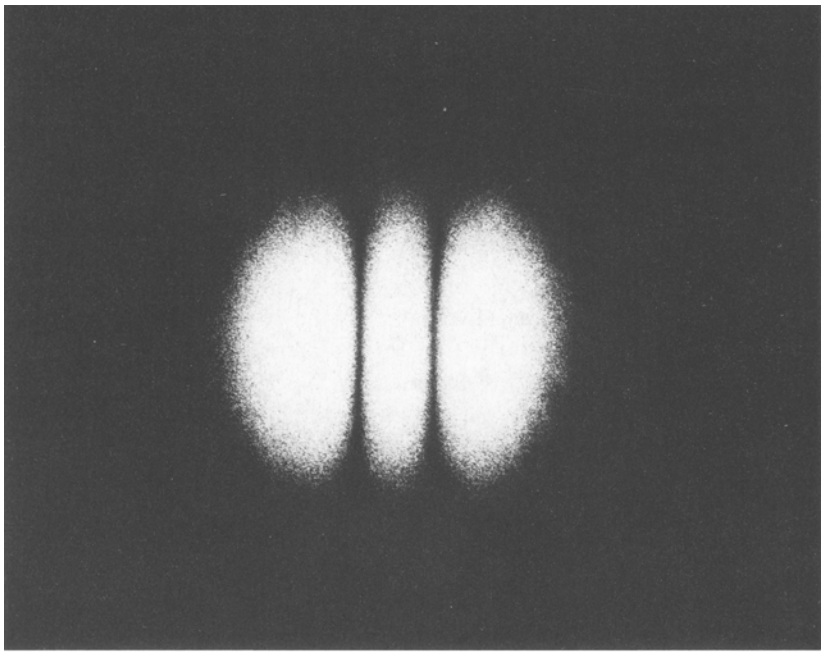

(c)

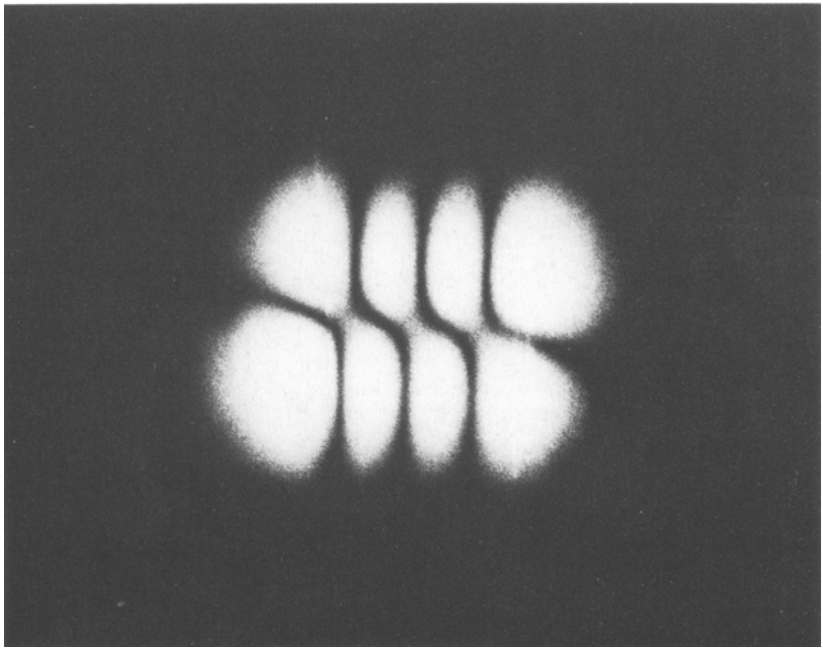

Fig. 5 (*continued*)

(d)

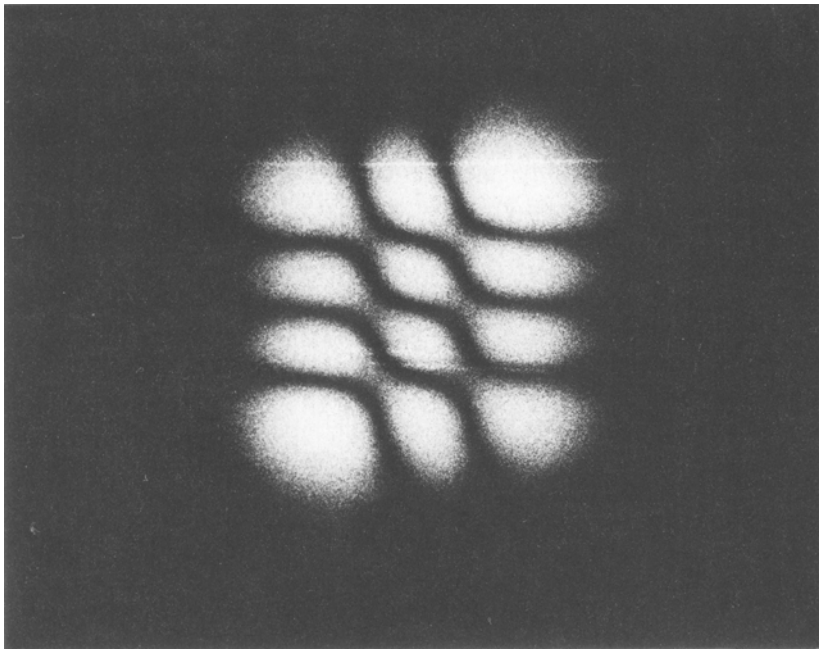

(e)

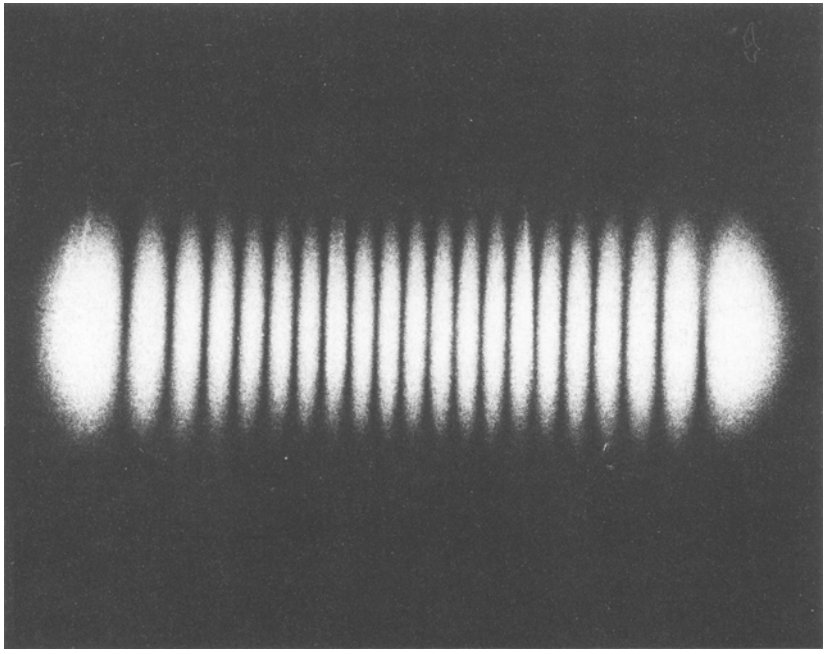

Fig. 5 (*continued*)

mination of the mode shapes; optical components at Brewster's angle also break the cylindrical symmetry. Consequently, the effect of rectangular symmetry is evident. These pictures were taken with the laser operating continuously in the steady state.

Though the existence of higher order transverse mode spatial patterns has been well known for many years, the dynamics of the formation of these patterns has not been studied, to our knowledge. We present here the results of an investigation of the transient dynamics of pattern formation. The technique used for this purpose is the measurement of first-passage-time distributions, which we used earlier with single-mode lasers to characterize the magnitudes and time scales of noise sources that induce fluctuations in lasers.[19] An acousto-optic modulator is used to Q-switch the dye ring laser while it is pumped by an argon ion laser. The time taken by the laser intensity to grow from the spontaneous emission background to a preset reference level is measured as shown in Fig. 1b. Repeated measurements of this first passage time are stored in a microcomputer and displayed in histogram form as a distribution. The FPT distributions measured for a single longitudinal and transverse mode laser (ref. 19) display a single peak that moves progressively to longer times as the reference level of the intensity (I_{ref}) is set closer to average steady-state intensity I_{ss}. Analysis of the shift and change in shape of the peak allows us to determine the characteristics of the noise sources that affect the growth of the laser radiation.

When the measurements of the FPT distributions of the single longitudinal and transverse mode laser were performed, it was noticed that occasionally the distributions obtained consisted of more than one peak. At first it was thought that these multiple peaks were due to the occurrence of more than one longitudinal mode. It rapidly became clear that if this was indeed the case, the coupling coefficients of the modes[22] must be extremely small, so that they could grow independently of each other.[23] At the same time, a calculation of the coupling coefficients between longitudinal modes of a unidirectional ring laser showed that the coupling would necessarily be strong, unlike in the case of the standing wave laser, where the existence of spatial hole-burning can lead to minimal coupling between modes.[24] The only possibility that remained was the existence of two *spatially distinct* modes that grew from the spontaneous emission background, and which utilized different regions (with little overlap) of the inverted active medium for gain (such as the TEM_{00} and TEM_{01} modes).

To verify this hypothesis, we monitored the spatial mode structure of the laser by expanding the beam with a short-focal-length lens. The FPT distributions shown in Fig. 6 are typical ones for the case of two coexisting modes that are only minimally coupled since they do not appreciably

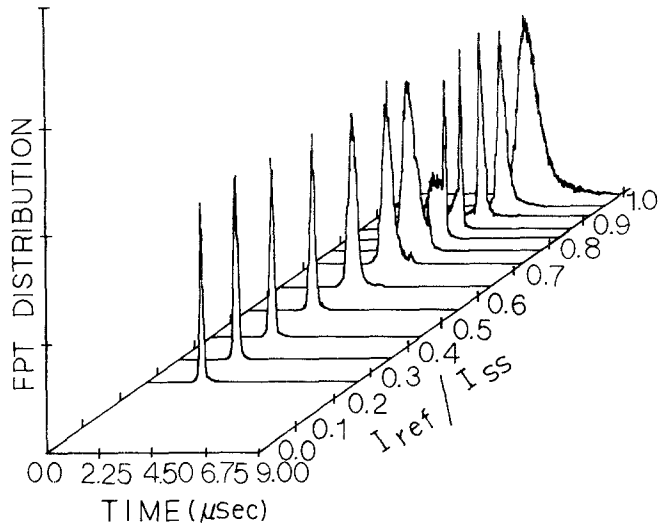

Fig. 6. Experimentally measured first-passage-time distributions for two coexisting transverse modes. The sequence of distributions corresponds to increasing values of the ratio of the reference intensity I_{ref} to the average steady-state intensity I_{ss}.

overlap in the dye medium. We have repeated the measurements many times to verify that multiple peaks in the FPT distributions occur only when two or more transverse modes coexist. The simplest situation is that of the two lowest order TEM modes, as mentioned earlier. The intensity trace for the initiation of the laser in this situation consists of a curve with a kink or plateau as shown in Fig. 7, where we have simulated the growth of the intensity for two uncoupled modes on the computer. This plateau on the intensity trajectories is responsible for the presence of the second peak in the FPT distributions that are measured for the appropriate values of I_{ref}/I_{ss}.

The equations for the time evolution of the two-mode laser are

$$\dot{E}_1 = a_1 E_1 - A_1 |E_1|^2 E_1 - \theta_{12} |E_2|^2 E_1 + p(t) E_1 + q_1(t) \tag{11}$$

$$\dot{E}_2 = a_2 E_2 - A_2 |E_2|^2 E_2 - \theta_{21} |E_1|^2 E_2 + p(t) E_2 + q_2(t) \tag{12}$$

where E_1 and E_2 are the complex fields of the two modes, a_1 and a_2 are the net gain coefficients, A_1 and A_2 are the saturation coefficients, θ_{12} and θ_{21} are the coupling coefficients,[22] and the noise parameters have been defined earlier.

In Fig. 8 we show Monte Carlo simulations of FPT distributions obtained from trajectories similar to those in Fig. 7 that qualitatively

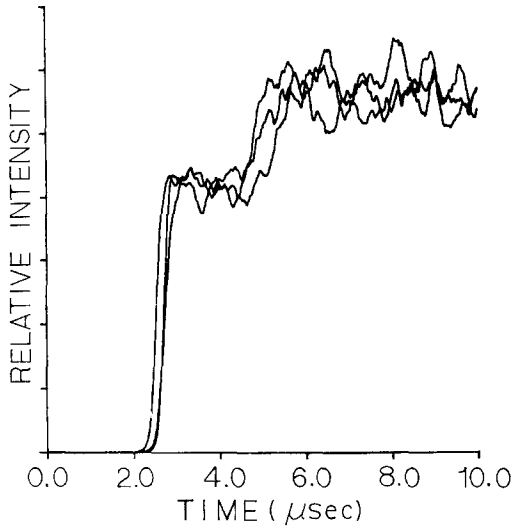

Fig. 7. Individual trajectories for the growth of the laser intensity as simulated from the equations for the fields of the two-mode laser.

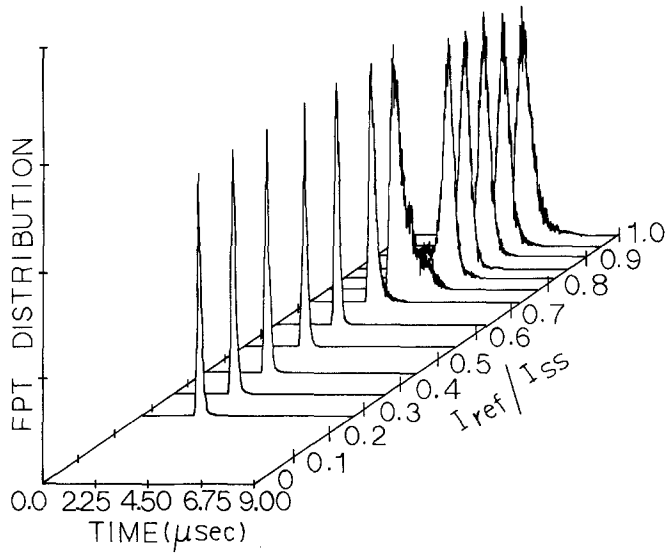

Fig. 8. First-passage-time distributions obtained from numerical simulations of the two-mode laser. The distributions are qualitatively similar to those of Fig. 6.

reproduce the experimentally measured ones of Fig. 6. The parameters assumed for the simulation are

$$a_1 = 6.9 \times 10^6 \text{ sec}^{-1} \qquad \theta_{12} = \theta_{21} = 0$$
$$a_2 = 3.5 \times 10^6 \text{ sec}^{-1} \qquad R_1 = R_2 = 1 \times 10^{-6} \text{ sec}^{-1}$$
$$A_1 = 6.5 \times 10^4 \text{ sec}^{-1} \qquad D = 2 \times 10^4 \text{ sec}^{-1}$$
$$A_2 = 1 \times 10^5 \text{ sec}^{-1} \qquad \Gamma_p = 6 \times 10^6 \text{ sec}^{-1}$$

These parameter values have not been selected by a systematic search procedure; they are merely estimates that produce qualitatively similar distributions to those determined experimentally. Ten thousand trajectories of 1000 time steps each were used in the simulations, each time step being 10 nsec. We note that the correspondence between the simulation and experiments is not quite perfect. We have assumed totally uncoupled modes in the calculations. Further, and more importantly, we have not accounted for the transverse dimensions in the calculations, but grossly simplified the task by accounting only for the time dependence of the amplitudes.

In reality, the modes do overlap to some extent, and there is some finite coupling between them. The inclusion of spatial dimensions is necessary if an attempt is to be made to reproduce the quantitative behavior of the modes. Thus, the results presented here are the simplest possible approximation to the study of the dynamics of spatial pattern formation in lasers.

An interesting feature of the simultaneous operation of the laser in two distinct spatial patterns is the possibility of lasing at two separate wavelengths. We are at present investigating the spectral behavior of the two modes experimentally. It was seen in our initial measurements that the laser may be bichromatic, with each of the two transverse modes lasing at a different wavelength. The conditions necessary for such phenomena are being explored in our laboratory. The broadband nature of the dye molecule energy levels is certainly involved in such bichromatic lasing, and a theory that incorporates this, such as that of Fu and Haken,[25] may be required to provide an accurate description of the laser.

5. DISCUSSION

The experiments on the power spectra of the single-mode ring dye laser demonstrate the critical slowing down of the laser as it is operated closer to threshold. The external pump noise serves as a probe of this behavior, and the response of the dye laser to the pump fluctuations is to act as a low-pass filter near threshold. An approximate theoretical analysis

is found to be reasonably accurate for operation of the laser fairly far above threshold, and computer simulations of the power spectra are compared with both the experiment and analytic approximation. It is seen that near threshold the power spectra calculated from simulations show significant differences from the analytic approximation. It should be noted that these measurements show a behavior of the power spectrum that is in agreement with a theoretical treatment by Sigeti and Horsthemle, who investigated power spectra for chaotic and noise-driven systems. The ring dye laser is an example of the latter. The transient digitizer used in these experiments limited us to eight bits of accuracy; we will investigate power spectra in the future with higher precision; the exact nature of the falloff of the spectra at high frequencies will then be better described.

The FPT measurements on the spatial patterns of the laser are the first investigation of the transient growth dynamics of the transverse modes that examine the effect of noise on the formation of the patterns. We have shown that these spatial modes develop in an almost uncoupled fashion and that their times of growth are different depending on the modes and the net gain experienced by them. Clearly, we need to extend our experimental techniques to obtain spatial resolution in our measurements (for example, a gated video camera will be necessary to discern details of the pattern formation) that presently are limited to a description only of the overall growth characteristics. The spectral content of the laser needs extensive study. Efforts to examine these aspects of spatial pattern dynamics are underway in our laboratory. At the same time it will be necessary to develop theoretical formalisms to describe these rich and complex phenomena in nonlinear systems driven by noise.

ACKNOWLEDGMENTS

The authors have benefited from many discussions with Ron Fox, Joe Haus, and Kurt Wiesenfeld. The work at Georgia Tech was supported by a grant from the U.S. Department of Energy, Office of Basic Energy Sciences, Chemical Sciences Division.

REFERENCES

1. K. Pearson, *Nature* **72**:294 (1905).
2. Lord Rayleigh, *Phil. Mag.* **10**:73 (1880).
3. S. Chandrasekhar, *Rev. Mod. Phys.* **15**:1 (1943).
4. L. Mandel and E. Wolf, eds., *Selected Papers on Coherence and Fluctuations of Light*, Vol. 1 (Dover, New York, 1970).
5. L. Mandel and E. Wolf, *Rev. Mod. Phys.* **37**:231 (1965).

6. M. Born and E. Wolf, *Principles of Optics*, 5th ed. (Pergamon Press, New York, 1975).
7. R. J. Glauber, *Phys. Rev.* **130**:2529 (1963).
8. R. J. Glauber, *Phys. Rev.* **131**:2766 (1963).
9. E. C. G. Sudarshan, *Phys. Rev. Lett.* **10**:277 (1963).
10. H. M. Nussenzveig, *Introduction to Quantum Optics* (Gordon and Breach, New York, 1973).
11. R. Loudon, *The Quantum Theory of Light*, 2nd ed. (Oxford University Press, New York, 1985).
12. R. Roy, A. W. Yu, and S. Zhu, in *Noise in Nonlinear Dynamical Systems*, F. Moss and P. V. E. McClintock, eds. (Cambridge University Press, 1988).
13. N. B. Abraham, *Laser Focus* **19**:73 (1983).
14. G. P. Agrawal and R. Roy, *Phys. Rev. A* **37**, to appear.
15. S. Machida, Y. Yamamoto, and Y. Itaya, *Phys. Rev. Lett.* **58**:1000 (1987).
16. D. Sigeti and W. Horsthemke, *Phys. Rev. A* **35**:2276 (1987).
17. A. W. Yu, G. P. Agrawal, and R. Roy, *Opt. Lett.* **12**:806 (1987).
18. J. M. Sancho, M. San Miguel, S. L. Katz, and J. D. Gunton, *Phys. Rev. A* **26**:1589 (1982).
19. S. Zhu, A. W. Yu, and R. Roy, *Phys. Rev. A* **34**:4333 (1986).
20. H. Kogelnik and T. Li, *Proc. IEEE* **54**:1312 (1966).
21. A. E. Siegman, *Lasers* (University Science Books, California, 1986).
22. M. Sargent, M. O. Scully, and W. E. Lamb, *Laser Physics* (Addison-Wesley, Reading, Massachusetts, 1982).
23. A. W. Yu, S. Zhu, R. Roy, M. Scalora, and J. W. Haus, paper TUF4, *International Laser Science Conference Technical Digest*, p. 24 (1986).
24. M. G. Raymer and M. Beck, Private communication.
25. H. Fu and H. Haken, *Phys. Rev. A* **36**:4802 (1987).